The crystal modulus and structure of oriented poly(ethylene terephthalate)

T. Thistlethwaite*, R. Jakeways and I. M. Ward
Department of Physics, University of Leeds, Leeds LS2 9JT, UK
(Received 17 February 1987; revised 12 June 1987; accepted 16 July 1987)

Crystal modulus measurements have been made on a number of samples of drawn poly(ethylene terephthalate) tape. The apparent crystal modulus was found to vary systematically with the degree of tilt of the crystalline *c* axis from the fibre axis. Using this fact, a value of 110 ± 10 GPa was deduced for the intrinsic crystal modulus in the chain direction. It is considered that this value is more realistic than previously reported values since specimen morphology has been taken into account carefully in a systematic fashion.

(Keywords: poly(ethylene terephthalate); morphology; crystal modulus; X-ray analysis)

INTRODUCTION

A number of previous experiments have reported measurements of the crystal modulus of poly(ethylene terephthalate) (PET) and there is some discrepancy between them. We have aimed to resolve the discrepancies by paying especial attention to the morphology of our samples and the way in which the morphology affects the relationship between the apparent crystal modulus and the true crystal modulus.

Dulmage and Contois[1] used a constant-strain technique and stresses between 100 and 200 MPa. They reported a value for the modulus in the chain direction of 137 GPa, but the problem with a constant-strain method is that it is difficult to take account of stress relaxation in the sample.

Sakurada and coworkers[2] used a dead-loading technique and even higher strains and reported a value of 75 GPa. A later paper[3] showed measurements on a sample of higher crystallinity and this estimate was revised to 108 GPa. In neither paper was specimen characterization considered in any detail, and the sample morphology was considered to correspond to a simple two-phase series layer structure.

Ovchinnikov[4] again used very high stresses and found a value of 75 GPa, rising to 133 GPa at high stresses when strain hardening was assumed to occur.

Three theoretical studies have been made of the stiffness of the PET polymer chain. Lyons[5] suggested a value of 146 GPa, Treloar[6] used a more refined method and gave 122 GPa and the most recent, by Tashiro *et al.*[7], put forward a figure of 95 GPa using a more sophisticated model than either of the other two.

In the present investigation a number of samples (about 20) of drawn PET fibre were prepared whose detailed morphologies were varied by subjecting them to differing annealing conditions.

Measurements were made of density, long period using SAXS, orientation of *c* axis to the fibre direction, mean crystallite size in the *c* axis direction, apparent crystal modulus and Young's modulus (the latter mainly at room temperature, but over a range of temperatures for a few of the samples).

The apparent crystal modulus (*ACM*) showed a small systematic variation with annealing conditions. The degree to which samples were annealed affected in particular the angle between the crystalline *c* axis and the fibre direction, and, as seen below, the response of the crystalline fraction to an applied macro-stress shows a small but significant dependence on this angle. It is shown that consideration of the angle of tilt is vital if one is to understand the deformation of the crystal unit under an applied macroscopic stress since, if polymer chains are *not* oriented along the fibre direction, then application of stress will have the effect of bringing about a partial reorientation as well as deforming the crystal itself. This leads to an underestimate of the crystal modulus when an attempt is made to deduce it from the apparent crystal modulus. Furthermore, the true crystal modulus can only be deduced from the apparent modulus if the morphology of the material is known, and we present evidence for a three-phase model as opposed to the simple series two-phase model which has been assumed in previous estimates of crystal modulus. The outcome of the work has been the deduction of a reliable and realistic value for the stiffness in the *c* direction of the PET crystalline unit. This value is in good agreement with recent theoretical values and we are confident that it can be used as a yardstick by which to judge the efficacy of any method used to manufacture high-modulus PET fibres.

EXPERIMENTAL

Specimen preparation

The starting material was undrawn PET sheet made by ICI Plastics Division, Welwyn Garden City. This was 0.85 mm thick and X-ray examination showed it to have an unoriented, amorphous morphology.

Dumbbell samples were cut from the sheet and drawn in an Instron tensile testing machine under a variety of conditions in order to find those conditions which, in combination with a suitable annealing treatment, would produce samples of high draw ratio, high crystalline orientation and high crystallinity. The best possible

* Present address: ICI Ltd, Agricultural Division, PO Box 6, Billingham, Cleveland TS23 1LB, UK

0032-3861/88/010061-09$03.00

samples in these respects were needed for the crystal modulus measurements.

The drawing conditions eventually used for producing the samples were: strain rate $\simeq 0.01\ s^{-1}$, draw temperature $\simeq 82°C$. These conditions gave a draw ratio of around 6, consistently, and the samples produced were then vacuum annealed to varying degrees of severity in order to produce specimens with the range of characteristics that we needed to carry out our investigations. Annealing was carried out, mostly under conditions when the sample was held at constant length, over the range from 4 h at 150°C to 27 h at 200°C.

Crystallinity

The crystallinity of each sample was estimated by measuring its density in a graded liquid column prepared using carbon tetrachloride and n-heptane. This allowed densities to be measured to an accuracy of about 0.1%.

Small-angle X-ray measurements (SAXS)

The existence of a distinct long period in the chain direction was investigated using SAXS. A point-focus Franks camera was used for this purpose and the resulting X-ray diffraction pattern consisted, in all cases, of a characteristic two-bar pattern. The Bragg equation was used to deduce the long period from this pattern. Although such a simple pattern does not unambiguously demonstrate the existence of a unique long period, it has been our experience that the procedure used is reasonable. Long exposures on drawn polyethylene samples have shown the existence of a second-order reflection and the long period deduced from the more complete data is identical with that deduced from the first-order reflection alone.

Crystal size measurements

Estimates of the crystal size, i.e. the mean coherence length of the crystalline portion in the chain direction, were made using the position-sensitive detector (see below). This was set up for high resolution, enabling X-ray linewidths down to about 0.2° in 2θ to be measured. The Scherrer equation was used to deduce the mean crystal length from the breadth of the $\bar{1}05$ reflections from each sample. An aluminium sample enabled us to determine the instrumental broadening, which allowed the raw linewidths to be corrected using a curve-fitting technique on a computer. An attempt was made to estimate the contribution to the linewidths of distortion broadening using the theory of Hosemann *et al.*[8] To this end additional measurements were made on the $\bar{1}03$ reflection for two samples of contrasting character. Although these two reflections do *not* represent different orders of reflection from the *same* crystal planes, it was thought that we should be able to discern any gross distortion broadening. In the event, the corrections to the crystal size suggested by the two sets of measurements were of the order of 10% and, bearing in mind the uncertainties involved in making such measurements on a polymer material, all subsequent calculations were performed using the crystal sizes deduced from the $\bar{1}05$ reflection only. Further reference to this will be made later.

Crystalline orientation

The next measurements required were those of crystalline orientation. The drawn samples were mounted horizontally on the diffractometer turntable and rotated about a vertical axis whilst the X-ray detector was held at the Bragg angle corresponding to the $\bar{1}05$ reflection. As the specimen rotated, the scattered intensity varied according to the distribution of $\bar{1}05$ plane normals about the draw direction.

Young's modulus

Young's modulus measurements were made using a constant-load creep apparatus in which a dead load is applied to a length of fibre or tape and the extension is measured by recording the motion of the lower end of the sample (see, for example, ref. 9). Ten second isochronal creep moduli were recorded at room temperature ($21 \pm 2°C$). Some selected samples were further investigated over a range of temperatures down to $-150°C$.

An important feature of such a technique is to ensure that the aspect ratio of the sample used is sufficiently high to reduce end effects to a minimum. This is especially important in very highly drawn tapes and fibres where there is a very high degree of mechanical anisotropy, e.g. ultra-high-modulus polyethylene and polypropylene. In the present work the modest draw ratios of little more than 6 produced samples of comparatively low mechanical anisotropy so that it was not necessary to employ very extreme aspect ratios.

The samples were produced in two groups. The first of these had cross-sections of 1.95 mm × 0.35 mm and the second 0.75 mm × 0.33 mm. Typical lengths used in the Young's modulus measurements were 40 mm for the first group (giving aspect ratios close to 20) and 30 mm for the second (giving aspect ratios of about 40).

Measurements of crystal modulus

Our aim was to make measurements at low stress levels that would enable us to obtain a reliable and accurate value for the crystal modulus. The general method has been described elsewhere[10-12] but the present measurements differ from those made previously in that a one-dimensional position-sensitive detector (PSD) was used to record diffraction profiles. The advantage of this device is that a complete profile can be recorded in a short time, in favourable cases in a matter of seconds, and a series of experiments can thus be completed in a brief enough time for experimental drift not to be troublesome.

The PSD was designed and constructed by the Rutherford Appleton Laboratory of SERC and consisted of a sealed gas counter with a sensitive area of some 10 × 2.5 cm. The detector is of the delay-line type in which an incoming X-ray photon sets off a highly localized electron discharge. This induces an electrical pulse in a delay line which is capacitively coupled to the cathode. A pulse travels in both directions along the delay line and the time difference between the arrivals of a pulse at either end is a measure of the position at which the X-ray discharge occurred. The spatial resolution of the detector is about 0.4 mm, a figure that was obtained by masking off all but a 0.1 mm wide area of the detector and measuring the response to a broad X-ray beam. When

used at some 270 mm from the specimen, the intrinsic resolving power of the detector is thus close to 0.1° in 2θ.

A diffraction profile is recorded by feeding the pairs of output pulses into a time-to-amplitude converter, the output pulses from which are stored in a pulse-height analyser (PHA). The contents of the PHA memory can be rapidly transferred onto a disc file of a microcomputer and the resulting data analysed at leisure either locally or with a mainframe computer.

Details of the detector are to be found in Bateman and Connolly[13,14]. The essence of the method that we use for measuring the apparent crystal modulus is that the sample is held in an extensometer which is mounted on the turntable of a conventional horizontal diffractometer (Philips type PW1380). The extensometer has been described previously[15].

A loading programme is applied to the sample of the kind: $L_0, L, L_0, 2L, L_0, 3L, \ldots$ where L_0 is a zero load. The diffraction profile is recorded each time and the centroid of the profile computed by a curve-fitting method in which the experimental data are fitted to a combination of mathematical functions such as Gaussian + Lorentzian- + background (see e.g. Bevington[16]). The method used was developed to be flexible and powerful and will cope with an incomplete diffraction profile such as is obtained when two overlapping reflections are present. This was not a problem in this work. The computing procedures produce numerical values for the uncertainties in the centroid positions which have been found to be comparable with the fluctuations recorded when a number of measurements of the same profile have been made in quick succession. It should be noted however that it was necessary to count for a long enough time for the intrinsic (statistical) uncertainty to be considerably less than the shift in centroid position which occurs on loading the sample. This intrinsic uncertainty is approximately equal to the standard deviation of the diffraction profile (treated as a Gaussian) divided by the square root of the total number of X-ray counts in the profile.

Details of the particular methods used in the current work will be found in Thistlethwaite[15].

The crystal structure of PET is well known (see, for example, Daubeny *et al.*[17]). The unit cell is triclinic (see *Table 2*) and the c axis is usually found to be inclined by up to some 6° or so to the draw direction in a drawn fibre or tape (see below).

One immediate problem in investigating PET is that there is no $00l$ reflection available which will give the length, and changes in the length, of the c axis directly. The $\bar{1}05$ reflection has to be used and the normal to this plane lies some 11.5° from the c axis. The $\bar{1}05$ plane spacing ($d_{\bar{1}05}$) can clearly be affected by changes in the a axis and in the three triclinic angles as well as by changes in the c axis. A calculation shows that variations in α and β are particularly significant and it is therefore necessary to address the question of whether, and under what conditions, such changes can occur.

First, if the c axis direction coincided with the fibre direction, then application of a tensile stress along this direction would produce extension along the c axis accompanied by a Poisson's ratio contraction of the other two axes. We have measured, using the same techniques as described above, the changes in lateral crystal dimensions under the application of a longitudinal stress and find:

$$v_{bc} = +0.7 \qquad v_{ac} = 0 \tag{1}$$

where v_{ij} represents the Poisson's ratio corresponding to the ratio of the contraction along the i axis to the extension along the j axis of the unit cell. Now when a chain extends under an applied load the angle α, for example, will increase since the next chain simply moves closer to the first. A calculation shows that a 1% change in c leads to a 0.7% change in b, which results in a calculated change in α of $\simeq 0.07\%$. The resulting change in the spacing of the $\bar{1}05$ planes, which is what we use to estimate the change in the c axis, is then calculated to be 0.03% from the change in α alone. Since v_{ac} is effectively zero we need not consider changes in $d_{\bar{1}05}$ arising from the Poisson's ratio deformation along the a axis. The conclusion therefore is that, if the c axis lies along the fibre direction, i.e. zero angle of tilt, then changes in the spacing of the $\bar{1}05$ planes arise principally from changes in the c axis dimension, and measurements on the $\bar{1}05$ reflection therefore enable us to deduce directly the c axis strain. However, we show below that the tilt is *not* zero in any of our samples, so we must consider the behaviour of the crystal unit when the c axis is inclined to the fibre direction. These tilt measurements show that the degree of tilt decreases when the fibre is stressed. The inclined crystal unit is clearly undergoing a change that might well include a change of shape, which is more complex than that considered above since the applied stress is no longer purely along the c axis. We thus expect the inter-axial angles to change by more than in the case of zero tilt and would expect to see a different relationship between changes in the $\bar{1}05$ plane spacing and changes in the c axis. If this is true then there should be a systematic variation in the apparent crystal modulus as the measured tilt angle varies. This is indeed the case, as is seen below.

RESULTS

Crystallinity

In order to estimate the crystallinity it is necessary to know (a) the density of the amorphous phase and (b) the density of the crystalline phase. The amorphous density was taken to be that of a specimen quenched from the melt and showing no trace of crystalline peaks in its X-ray diffraction pattern. The ρ value we used in the current work was 1335 kg m^{-3}.

The crystal density is a little more difficult since it requires very accurate values of the six lattice parameters. The early measurements of Daubeny *et al.*[17] are frequently used but the measurements of Northolt and Stuut[18] are more sophisticated and take into account the variation of the structure factor across the profile of a reflection. The resulting densities are 1455 kg m^{-3} (ref. 17) and 1529 kg m^{-3} (ref. 18) and it is clear that the density used can considerably affect the crystallinity deduced using a simple two-phase model. The existence of a possible third phase, see e.g. Farrow and Ward[19] and Fischer and Fakirov[20], further confuses the issue and means that it is not possible, unambiguously, to deduce a realistic figure for crystallinity from density measurements alone. Later, we use the measured density figures to

Table 1 Sample draw ratios, annealing conditions, mean crystallite length and long periods

Specimen	Draw ratio	Annealing temp. (°C)	Annealing time (h)	Mean crystallite length ($\bar{1}05$) (Å)	Long period (Å)	ϕ = Mean crystallite length ÷ Long period
A	5.80			48	–	–
B	5.45	150	4	48	100	0.48
C	5.41	160	4	50	103	0.49
D	5.49	170	4	48	103	0.47
E	5.33	180	4	47	109	0.50
F	5.41	190	4	55	109	0.50
G	5.39	200	4	56	112	0.50
H	5.33	210	4	61	118	0.52
I	5.5[a]	200	14.5	67	116	0.58
J	5.34	200[b]	18	61	–	–
K	5.5[a]	200[b]	14.5	57	112	0.51
L	5.23	200	18	58	113	0.51
M	6.09	200	20	68	123	0.55
N	5.5[a]	200	15	80	120	0.67
P	6.0[a]	200	24	80	118	0.68
Q	5.6[a]	200	18	80	119	0.67
R	6.29	200	27	70	116	0.60
S	5.5[a]	200	17.5	72	119	0.60
T	6.0[a]	200	25	87	120	0.73
U	5.45	200	18	77	121	0.64
V	6.0[a]	200	25	87	122	0.71

[a] Nominal
[b] Annealed free

form a judgement as to the nature of the model that is most appropriate for our drawn tapes.

Long period

The deduced values of long period varied from about 100 to 120 Å and generally showed an increase as the annealing temperature was raised. These figures, and the observed trend, agree with results obtained by previous workers, e.g. Fischer and Fakirov[20], Statton and Goddard[21] and Yeh and Geil[22].

Crystal size

The mean crystal length in the c direction generally increased from around 50 Å for the least severely annealed specimens to nearly 90 Å for the most severely annealed samples. *Table 1* shows the results for the full set of samples together with values for the long period and the ratio of the mean crystal length to the long period, ϕ, which is referred to later in the discussion on the possible structure of the samples.

Crystalline orientation

Crystalline orientation measurements are complicated in PET since there is no true azimuthal reflection available in the diffraction pattern. The $\bar{1}05$ reflection lies close to the azimuth and an orientation scan performed as described above results in a pair of orientation curves which, generally, overlap. The experimental data points were computer fitted to a function consisting of two identical Gaussian curves added to a constant background. The fitting procedure produced a best-fit separation of the two Gaussian curves which was found to be accurate, and repeatable, to about 0.01°. The uncertainty in the resulting value of χ was thus taken to be equal to this figure. *Figure 1* shows two representative scans for a well oriented sample. The separation of the two curves should be $2 \times 11.56°$ if the unit cell of Northolt and Stuut is used, and it is an interesting feature of our work that the measured separation ($=2 \times \chi_{(\bar{1}05)}$) was always *less* than this. The implication is therefore either that the unit-cell dimensions vary from sample to sample as assumed, for example, by Bhatt, Bell and Knox[23], or that the variation arises from the fact that the c axis does not coincide in direction with the draw, or fibre, direction, as assumed by, for example, Casey[24].

In order to investigate which is the more likely possibility, the unit-cell parameters were measured, using an accurately set up scanning diffractometer, together with a unit-cell refinement program, for two samples (F and T) whose orientation curve separation angles differed by almost a factor of 1.5. *Table 2* shows the results of these measurements and *Table 3* shows the ($\bar{1}05$) peak separation angle for the whole range of samples.

The differences between the calculated separation angles for the two chosen samples are within the experimental error and are very much smaller than the variations in the experimentally observed values. We conclude therefore that, in general, the c axis is tilted from the fibre direction and the degree of tilt depends on the annealing conditions.

The degree of orientation of the crystals deduced by applying a curve-fitting program to the raw data was generally high. By degree of orientation we mean the orientation of the crystalline c axis about the direction of tilt and it is clear that one of the peaks in, for example, *Figure 1* shows a very close representation of this orientation distribution. The widths at half height of these peaks varied from 7° or so to about 13°, with the greater degree of orientation occurring in the least annealed samples.

This high degree of orientation meant that no corrections for orientation had to be incorporated into the work on crystal modulus described later. (A correction for tilt was, of course, made.)

One particular set of samples, B to H inclusive, was chosen with a view to investigating how annealing

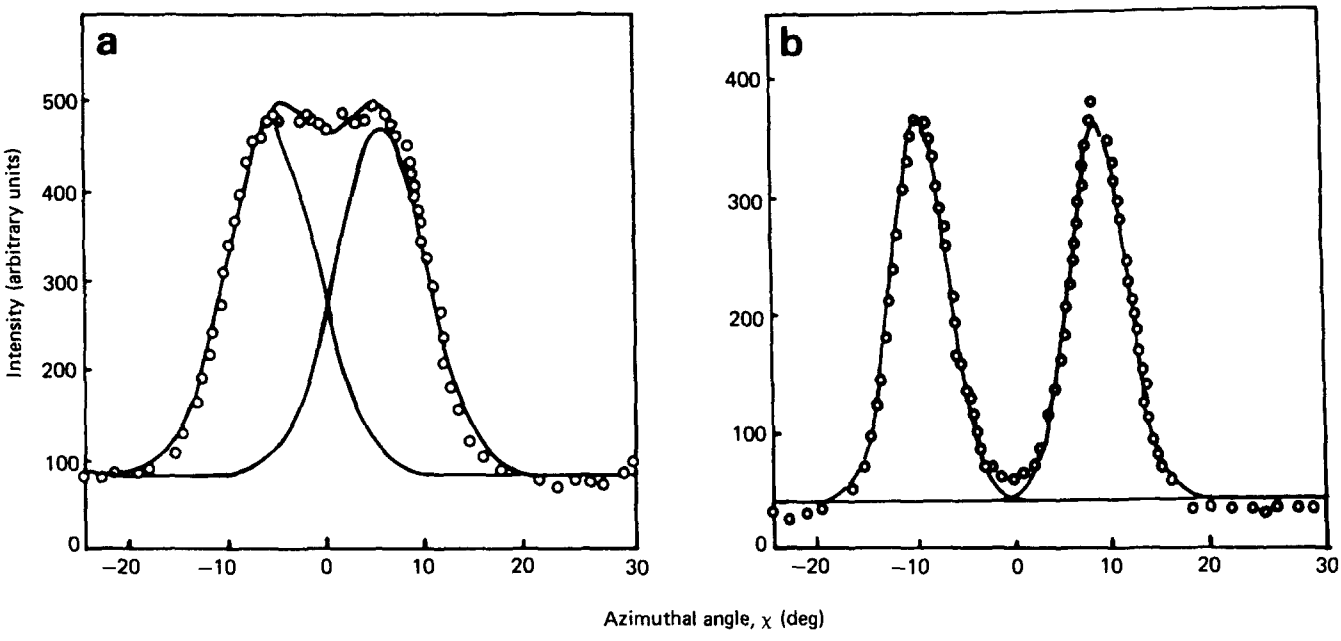

Figure 1 Azimuthal intensity profiles of the ($\bar{1}$ 0 5) reflection of (a) sample F and (b) sample T: ○, raw data; ———, fitted Gaussian components and their sum

Table 2 Unit-cell determination of samples F and T

(a) Peak positions

Index of reflection ($h k l$)	2θ (deg)	
	Sample F	Sample T
0 1 0	17.45	17.78
$\bar{1}$ 1 0	22.96	23.03
1 0 0	25.78	25.99
0 $\bar{1}$ 1	16.48	16.34
$\bar{1}$ 1 1	21.66	21.57
1 $\bar{1}$ 1	–	27.91
$\bar{1}$ 1 2	25.03	25.09
$\bar{1}$ 0 3	26.36	26.41
$\bar{1}$ 0 5	43.01	42.99

(b) Results of cell refinement

Sample	Unit-cell parameter					
	a (Å)	b (Å)	c (Å)	α (deg)	β (deg)	γ (deg)
F	4.54 ±0.03	5.87 ±0.03	10.71 ±0.06	99.1 ±0.6	119.2 ±0.5	110.1 ±0.5
T	4.53 ±0.04	5.87 ±0.05	10.73 ±0.1	99.6 ±1.0	119.1 ±0.3	110.6 ±0.8

Table 3 Crystallite orientation distribution: results of curve fitting

Sample	Halfwidth of ($\bar{1}$ 0 5) component (deg)	$\chi(\bar{1}\,0\,5)$ (deg)
A	13.42	7.21
B	13.71	5.75
C	12.43	5.93
D	12.86	5.48
E	12.85	5.99
F	12.36	6.26
G	11.93	6.30
H	12.36	6.44
I	11.79	6.72
J	12.15	6.41
K	12.31	6.06
L	12.50	5.95
M	12.29	8.06
N	9.11	8.43
P	8.40	8.46
Q	8.12	8.76
R	11.59	7.37
S	12.01	7.22
T	7.04	9.45
U	9.40	8.51
V	7.56	9.33

temperature affects morphological properties. Sample density was found to increase with the annealing temperature (see *Figure 2*). *Table 1* shows that the long period also shows a consistent increase as the annealing temperature is increased.

The tilt of the c axis is also correlated with temperature, as shown in *Figure 3*, higher annealing temperatures leading to the c axis lying closer to the fibre direction (smaller tilt, larger value of $\chi_{(\bar{1}\,0\,5)}$). No other mechanical or structural characteristics showed any systematic variation with annealing temperature.

Young's modulus measurements

Table 4 shows the variation of the 10 s creep modulus at

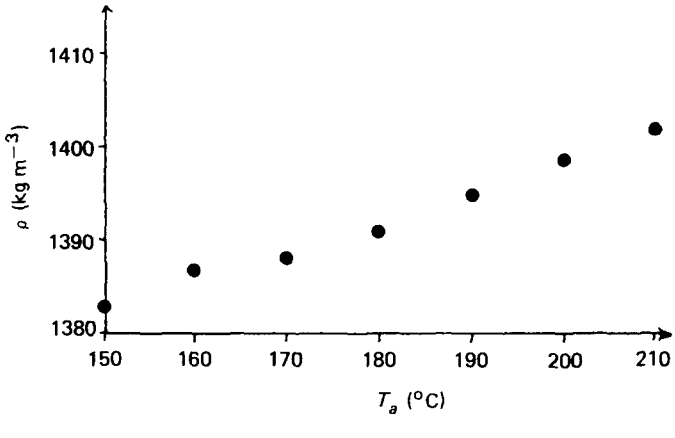

Figure 2 Density *versus* annealing temperature for samples B–H

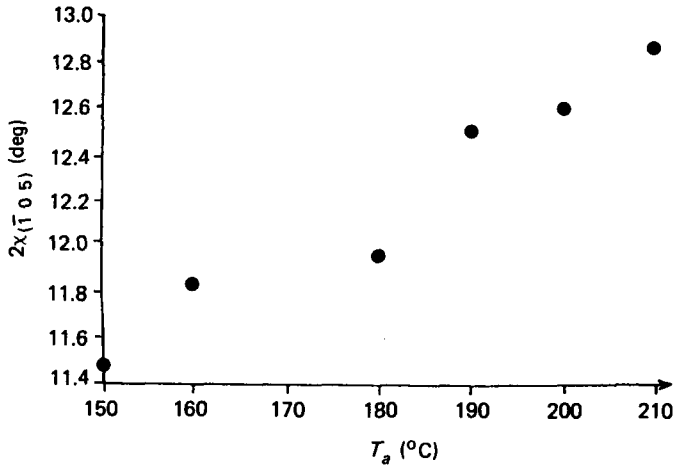

Figure 3 Azimuthal separation of $\bar{1}05$ peaks *versus* annealing temperature for samples B–H

Table 4 Ten second creep moduli – room temperature

Sample	Ten second creep modulus (GPa)
A	8.6
B	5.2
C	6.1
D	5.5
E	5.9
F	5.9
G	5.4
H	5.5
I	7.8
J	6.8
K	7.3
L	6.1
M	7.3
N	12.4
P	10.1
Q	6.7
R	7.0
S	9.2
T	13.2
U	8.0
V	12.4

room temperature for the range of samples studied. Moduli are not particularly high but are quite typical for specimens produced in this fashion.

Figure 4 shows the variation with temperature for five samples and it is notable that there is comparatively little variation over the temperature range studied. This has implications for a structural model, which are examined below.

Crystal modulus measurements

The experimental data yielded a stress–strain curve for each sample which related applied stress on the fibre to strain as determined by the $\bar{1}05$ plane spacing. Maximum stresses of up to 200 GPa were applied and there was no evidence of non-linearity for any of the samples. The slope of the curve gives a modulus figure for the $\bar{1}05$ plane normal which has to be corrected to relate it to the strain in the *c* axis. A straightforward calculation shows that a 1% strain in the *c* dimension leads to a 1.068% strain in the $\bar{1}05$ plane spacing. Hence, as a good approximation, i.e. ignoring any change arising from a change in α, which has been shown above to be small, the raw *ACM* pertaining to the *c* axis is found by multiplying the slope of the experimental stress–strain curves by 1.068. A series of values was deduced for the 21 samples, which had a mean of 74.1 GPa and a standard deviation of 5.1 GPa. There was no clear-cut trend and the standard deviation was comparable with the estimated experimental error of a single measurement. The magnitude of the experimental error was estimated from an assessment of errors in stress measurement, cross-sectional area of the specimen, thermal fluctuations and a consideration of the random statistical errors inherent in the deduction of the shift in the diffraction peak under load. Overall this assessment led to a general error level of around 10% for all measurements of the *ACM*.

Table 5 shows the results of making measurements on five samples over a range of temperatures. Again no trend is discernible, in sharp contrast to what is seen in polyethylene[10] and polyoxymethylene[12].

The question of the effect of tilt has already been discussed and it was mooted that the effect of an applied stress on the *c* axis dimension might well depend on the degree of tilt. *Figure 5* shows the *ACM* plotted against χ.

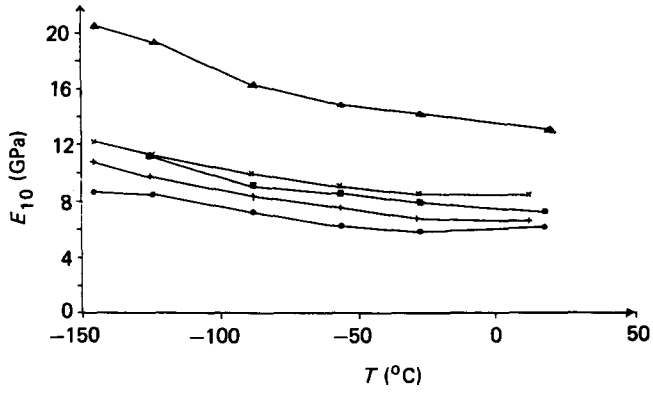

Figure 4 Variation of 10 s creep modulus E_{10} with temperature: +, sample Q; ×, sample A; ●, sample F; ▲, sample T; ■, sample M

Table 5 Low-temperature measurements of apparent crystal modulus (*ACM*)

Sample	Temperature (°C)	*ACM* (GPa)
Q	20	80
	−26.8	81
	−55.9	77
	−87.9	77
	−124.4	83
	−164.1	81
A	20	68
	−26.8	66
	−55.9	74
	−87.9	71
	−124.4	73
	−164.1	75
F	20	70
	−124.4	65
	−164.1	67
M	20	75
	−145.3	81
T	20	80
	−124.4	83

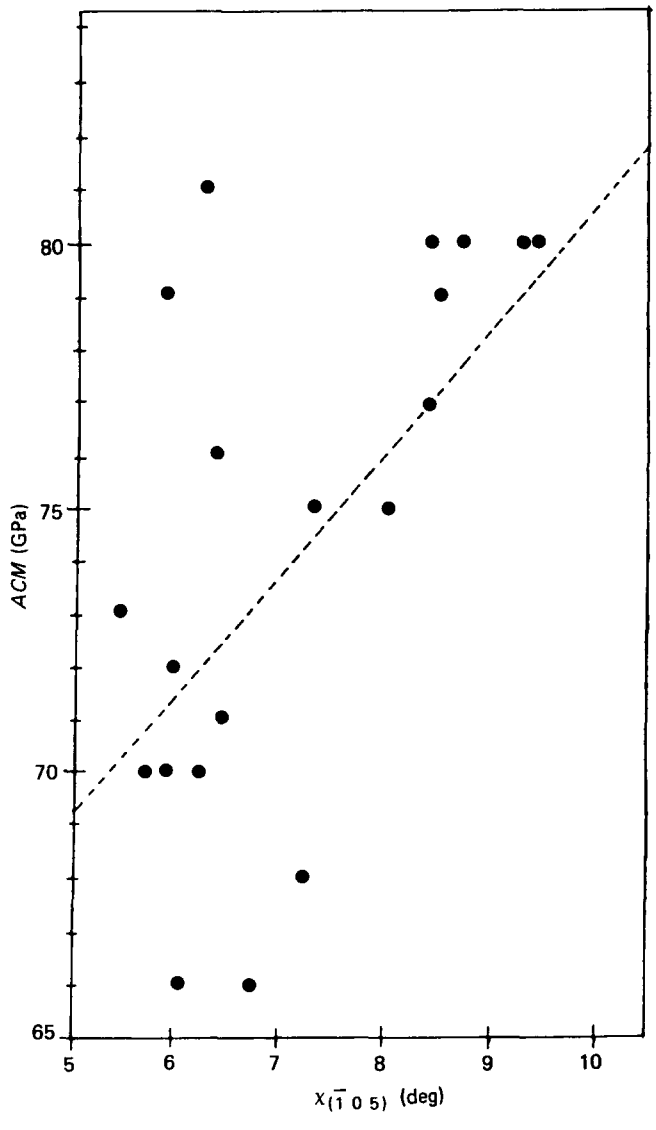

Figure 5 The correlation between $\chi(\bar{1}\ 0\ 5)$ and apparent crystal modulus (*ACM*)

There is no *strong* trend but analysis shows a significant correlation between the two variables.

Now the uncertainty in χ is *very* much less than the uncertainty in the *ACM* and hence the appropriate statistical analysis consists of a correlation of *ACM* on χ. The result of this correlation, which has a correlation coefficient of 0.56, has the form:

$$ACM = 2.31\chi_{(\bar{1}\,0\,5)} + 57.6\ \text{GPa} \qquad (2)$$

If this is now used to correct the observed values to zero tilt ($\chi_{(\bar{1}\,0\,5)} = 11.56°$), where little contribution is expected from anything other than *c* axis extension, then a value of *ACM* of 84.3 ± 4 GPa results. We regard this figure as relating to the true extension of the *c* axis but there still remains the question of whether the stress transmitted to the crystalline unit is the same as the applied mechanical stress or whether it differs from this, and if so, by how much. Resolution of this question will depend on a knowledge of the microstructure of the material.

DISCUSSION

In a simple series model the stress on the crystal unit would equal the applied stress and the true value of the crystal modulus would equal the *ACM* as derived so far. If the fibre is modelled by anything more complex then, in general, the stress on the crystal will be greater than the applied stress since there is usually some degree of stress concentration on the stiffer structural elements.

In a simple series model, consisting of crystalline blocks separated by disordered layers, we should expect to see a simple relationship between certain structural parameters, viz. crystallinity, long period and mean crystallite size in the fibre direction. This relationship in its most naive form would be:

$$\text{Degree of crystallinity} = \frac{\text{Mean crystallite length}}{\text{Long period}} \qquad (3)$$

Figure 6 shows crystallinity, as deduced from density, plotted against the right-hand side of the above equation using the lattice parameters, and hence the crystal density, measured by Northolt and Stuut[18]. It is evident that the above simple relationship does not hold in this case. It is interesting, but probably purely fortuitous, that if the earlier unit-cell of Bunn *et al.*[17] is used, the data points do, in fact, lie close to the series model line (45°) but, since we regard the Northolt parameters as far more realistic, we are confident that our data do not fit a series model.

We therefore propose a parallel–series model of the form shown in *Figure 7* to represent our PET fibres, which corresponds to that considered by Prevorsek *et al.*[25] in other PET studies. A simple calculation, as below, enables the degree of stress concentration on the crystal to be calculated and hence the true crystal modulus to be deduced.

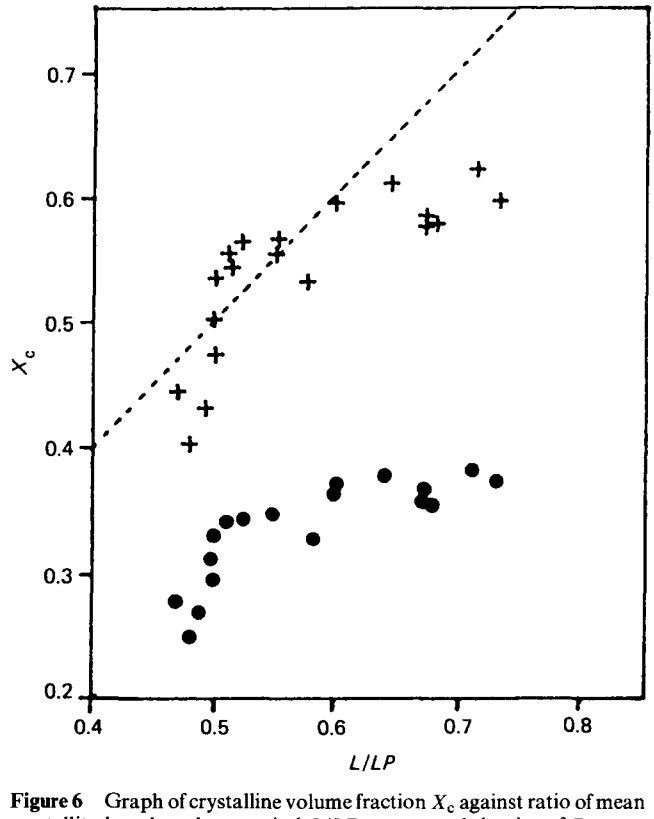

Figure 6 Graph of crystalline volume fraction X_c against ratio of mean crystallite length to long period *L/LP*: +, crystal density of Bunn *et al.*[17]; ●, crystal density of Northolt and Stuut[18]; -----, line corresponding to series model

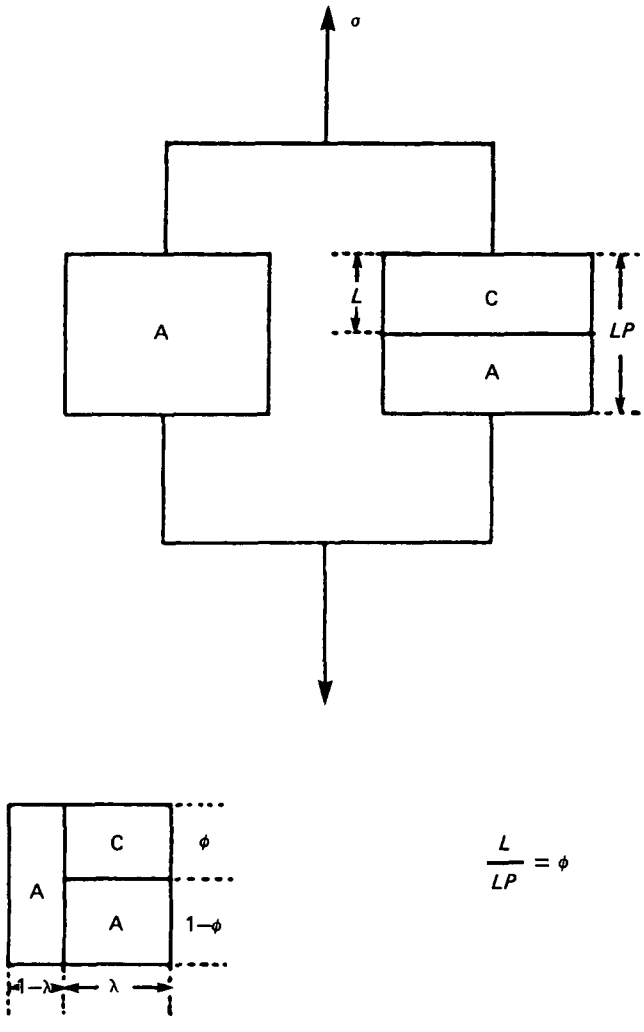

Figure 7 The parallel–series model; expressions for E_Y and ACM are given in equations (4) and (5)

If ϕ is defined as the ratio of mean crystallite length to long period and λ as (crystallinity/ϕ) then the relationship between ACM and the true crystal modulus E_c is:

$$ACM = (1-\lambda)[(1-\phi)E_c + \phi E_a] + \lambda E_c \quad (4)$$

where E_a is the Young's modulus of amorphous PET.

In addition the Young's modulus of the fibre is given by

$$E_Y = (1-\lambda)E_a + \frac{\lambda}{\phi/E_c + (1-\phi)/E_a} \quad (5)$$

Values of ACM and measured Young's modulus were inserted into the above equations and they were then solved for E_c and E_a. *Table 6* summarizes the data for all of the samples and we deduce from these data that the true, corrected value of the crystalline modulus of PET is 110 ± 10 GPa. It is important to note that the values of E_a fall within the range 3.33 to 9.10 MPa, which is a realistic range for an oriented amorphous polymer[26].

Low-temperature values were also inserted into the above equations and *Table 7* shows that the expected stiffening of the amorphous phase produces very little effect on the calculated crystal modulus. This lack of variation with temperature is also reflected in the experimental values of the ACM.

CONCLUSIONS

A comprehensive study of a number of PET fibres having different morphological characteristics has led to an understanding of the structure of the fibres and to an insight into the way that an applied stress leads to crystalline deformation. Measurements of that deformation has led to a value for the intrinsic stiffness of the PET crystal in the chain direction of 110 GPa, and we consider that this value is more reliable than previously

Table 6 The parallel–series model: calculated values of true crystal and amorphous moduli, based on the value of ACM corrected for the effect of detilting

Specimen	Corrected ACM (GPa)	Measured E_Y (GPa)	Measured ϕ	Measured λ	Calculated E_c (GPa)	Calculated E_a (GPa)
A	78	8.59	–	–	–	–
B	83	5.22	0.48	0.52	106.8	3.60
C	83	6.07	0.49	0.55	105.3	9.10
D	87	5.53	0.47	0.57	108.1	3.78
E	85	5.85	0.43	0.67	98.4	4.02
F	82	5.93	0.50	0.62	100.3	3.77
G	94	5.36	0.50	0.66	112.6	3.33
H	83	5.54	0.52	0.67	99.5	3.35
I	77	7.79	0.58	0.58	101.1	4.59
J	88	6.79	–	–	–	–
K	79	7.27	0.51	0.65	95.2	4.54
L	92	6.08	0.51	0.66	110.5	3.71
M	83	7.28	0.55	0.64	102.4	4.26
N	87	12.40	0.67	0.54	122.9	6.89
P	84	10.07	0.68	0.53	121.1	5.06
Q	86	6.68	0.67	0.54	122.8	3.33
R	85	6.99	0.60	0.60	110.6	3.84
S	78	9.24	0.61	0.61	100.8	5.03
T	85	13.20	0.73	0.51	128.9	6.10
U	86	8.00	0.64	0.59	115.1	4.11
V	85	12.35	0.71	0.54	123.4	5.80

Table 7 Calculations of true crystal and amorphous moduli at ambient and low temperature using the parallel–series model

	Measured macroscopic Moduli (GPa)		Measured *ACM* corrected for tilting		Calculated true crystal moduli (GPa)		Calculated amorphous moduli (GPa)	
Specimen	20°C	−124.4°C	20°C	−124.4°C	20°C	−124.4°C	20°C	−124.4°C
F	5.93	8.52	82	77	100	94	3.8	5.5
Q	6.68	9.91	86	89	123	126	3.3	5.0
T	13.20	19.44	85	88	129	132	6.1	9.4

reported values owing to the careful consideration of specimen morphology that has gone into its deduction. There is also encouragingly good agreement with the value of 95 GPa calculated by Tashiro *et al.*[7]

The work has also shown that, in general, when measuring the stiffness of an oriented semicrystalline polymer using a non-(00*l*) reflection, and more particularly when evidence exists for the systematic tilt of *c* axes to the draw direction, that extra consideration must be given to the lateral and angular deformations of the crystal unit cell.

REFERENCES

1 Dulmage, W. J. and Contois, L. E. *J. Polym. Sci.* 1958, **28**, 275
2 Sakurada, I., Ito, T. and Nakamae, K. *J. Polym. Sci. (C)* 1966, **15**, 75
3 Sakurada, I. and Kaji, K. *J. Polym. Sci. (C)* 1970, **31**, 57
4 Ovchinnikov, V. A., Zhorov, V. A. and Baskaev, Z. P. *Polym. Mech. (USA)* 1976, **8**, 868
5 Lyons, W. J. *J. Appl. Phys.* 1958, **29**, 1429
6 Treloar, L. R. G. *Polymer* 1960, **1**, 95, 279
7 Tashiro, K., Kobayashi, M. and Tadokoro, N. *Macromolecules* 1977, **10**, 413
8 See Alexander, L. 'X-ray Diffraction Methods in Polymer Science', Wiley, New York, 1969
9 Morgan, C. J. and Ward, I. M. *J. Mech. Phys. Solids* 1971, **19**, 165
10 Clements, J., Jakeways, R. and Ward, I. M. *Polymer* 1978, **19**, 639
11 Brew, B., Clements, J., Davies, G. R., Jakeways, R. and Ward, I. M. *J. Polym. Sci.* 1979, **17**, 351
12 Jungnitz, S. J., Jakeways, R. and Ward, I. M. *Polymer* 1986, **27**, 1651
13 Bateman, J. E. and Connolly, J. F. *Nucl. Instrum. Meth.* 1980, **173**, 525
14 Rutherford and Appleton Laboratories, Publication RJ-81-012
15 Thistlethwaite, T. Ph.D. Thesis, University of Leeds, 1985
16 Bevington, P. R. 'Data Reduction and Error Analysis', McGraw-Hill, New York, 1969
17 Daubeny, R. de P., Bunn, C. W. and Brown, C. J. *Proc. R. Soc. (A)* 1954, **226**, 531
18 Northolt, M. G. and Stuut, H. A. Preprint, AKZO Research Laboratories, Arnhem, The Netherlands
19 Farrow, G. and Ward, I. M. *Polymer* 1964, **1**, 320
20 Fischer, E. W. and Fakirov, S. *J. Mater. Sci.* 1976, **11**, 1041
21 Statton, W. G. and Goddard, G. M. *J. Appl. Phys.* 1957, **28**, 1111
22 Yeh, G. S. Y. and Geil, P. H. *J. Macromol. Sci.–Phys. (B)* 1967, **1**, 251
23 Bhatt, G. M., Bell, J. P. and Knox, J. R. *J. Polym. Sci., Polym. Phys. Edn.* 1976, **14**, 373
24 Casey, M. *Polymer* 1977, **18**, 1219
25 Prevorsek, D. C., Tirpak, G. A., Harget, P. J. and Reimschuessel, A. C. *J. Macromol. Sci. (B)* 1974, **9**, 733
26 Ward, I. M. 'Mechanical Properties of Solid Polymers', 2nd Edn., Wiley, Chichester, 1983, p. 294